electrochem

MDPI

Article

Electrochemical Sensing of Amoxicillin Drug-Assisted Uropathogenic *E. coli* Bacteria Using Gold Nanostructures—A Preliminary Study

Jayaprakash Sushmitha [1] and Subramanian Nellaiappan [1,2,*]

[1] School of Chemical and Biotechnology, SASTRA Deemed University, Thanjavur 613401, Tamil Nadu, India
[2] Srinivasa Ramanujan Centre, SASTRA Deemed University, Kumbakonam 612001, Tamil Nadu, India
* Correspondence: nellaiappan.s@scbt.sastra.edu

Abstract: The present study focuses on the electrochemical sensing of amoxicillin (AMX, as a model antibiotic drug) and its interaction with Uropathogenic *E. coli* (UPEC) bacteria (as a model pathogen) under physiological conditions. The electrochemical sensor probe is formulated by nanostructured gold wires (AuNWs) embedded in a carbon nanofiber–chitosan (CNF-CHIT) matrix. The synthesis of AuNWs is characterized by scanning electron microscopy (SEM), UV-Visible spectrophotometry, and X-ray photoelectron spectroscopy (XPS). The CNF-CHIT/AuNW-modified system is characterized by SEM and XPS. Initially, the CNF-CHIT/AuNW electrode was utilized for the sensing of AMX; later, in the antibiotic drug-assisted sensing of UPEC, i.e., in the presence of AMX, the interaction of UPEC was studied. The modified electrode showed appreciable sensitivity for AMX sensing; also, the interaction of AMX with UPEC is studied at two different conditions. One, at a fixed concentration of AMX (100 µM) and different concentrations of UPEC bacteria (0.6–1.2 × 10^6 CFU/mL), and another with incubation time (1 h–1 h 35 min) for bacterial reaction. The electrochemical antimicrobial resistance developed by UPEC, which is inherent in the sensing of AMX, is the key concept for the detection of pathogens.

Keywords: urinary tract infection; gold nanostructures; amoxicillin; uropathogenic *E. coli*; electrochemical sensor

check for updates

Citation: Sushmitha, J.; Nellaiappan, S. Electrochemical Sensing of Amoxicillin Drug-Assisted Uropathogenic *E. coli* Bacteria Using Gold Nanostructures—A Preliminary Study. *Electrochem* **2023**, *4*, 291–300. https://doi.org/10.3390/electrochem4020020

Academic Editors: Masato Sone and Michael Fowler

Received: 9 May 2023
Revised: 2 June 2023
Accepted: 12 June 2023
Published: 13 June 2023

Copyright: © 2023 by the authors. Licensee MDPI, Basel, Switzerland. This article is an open access article distributed under the terms and conditions of the Creative Commons Attribution (CC BY) license (https://creativecommons.org/licenses/by/4.0/).

1. Introduction

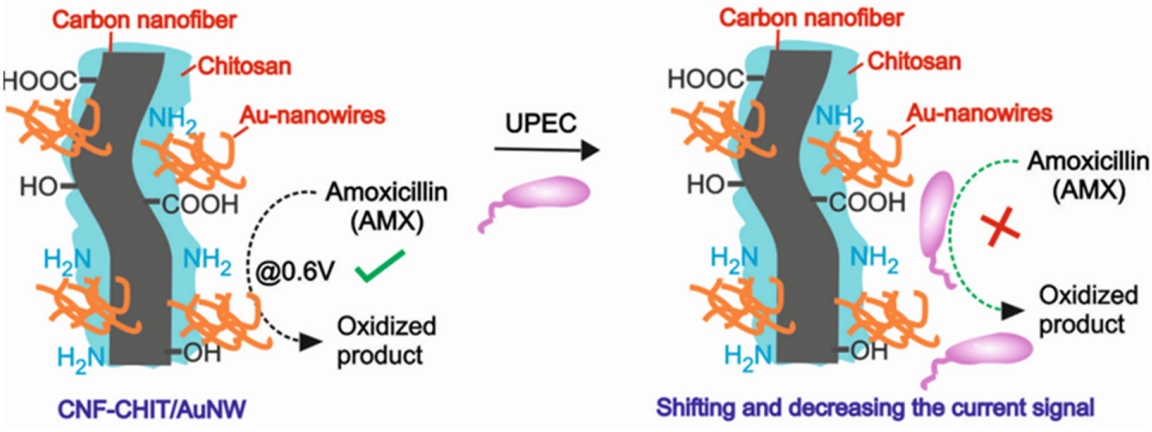
Urinary tract infection (UTI) is the most commonly occurring infectious disease, yet it is not considered to be a serious condition. The fatality related to this condition is not as high as other fatal diseases but highly affects one's quality of life in different ways. It affects almost 50% of the population [1], leading to an increased risk of bacteremia and septicemia. In a study with 500 patients, it was found that 76.80% reported having complicated UTIs, while 88.20% reported having community-acquired UTIs. It was also found that 8.40% accounted for catheter-related infections. From the study, it was evident that the most common infection-causing bacteria in the case of UTI was *Escherichia coli*, with an occurrence of 57.03% in complicated and 55.17% in uncomplicated UTIs [2–4]. The bacterial infection causes pyelonephritis, cystitis, urethritis leading to renal failure, tumors in the urinary tract, bacteremia (in the bloodstream), and septicemia (inflammatory response), which becomes a fatal condition for the female population [5]. This frequently occurring bacterial infection is reported to cause 150 million cases per year. Furthermore, 50–60% of women are estimated to be infected at least once in their lifetimes [6,7]. Even though this infectious condition is not considered to be serious and fatal, not treating it at the right time leads to a troubled lifestyle, leading to increased possibilities of fatality.

The conventional diagnostic method includes urine culture and dipstick urinalysis [8,9]. Dipstick analysis takes 1–2 min, but the accuracy is highly compromised. In this method, the presence of leukocyte esterase and nitrates are estimated. A urine

culture is performed to culture the sample infected with bacterial strains. In this case, the specificity and accuracy are high, wherein the bacterial species causing the infection can be identified. Even though these methods are sensitive and selective, they require complex steps, skilled personnel, and time-consuming analysis (~48–72 h), which are not suitable for point-of-care diagnosis. The electrochemical detection method seems to be a convincing factor, with the ease of fabrication of electrodes and point-of-care devices [10,11]. Recently, a series of electrochemical immune/biosensors based on DNA [12–14], antibodies [15–17], aptamers [18–21], antimicrobial peptides [22], lectin [23], carbohydrates [24], and bacteriophages [25] for the detection of *E. coli* bacteria have been studied by using differential pulse voltammetry (DPV) [12,13,17,18], electrochemical impedance spectroscopy (EIS) [15,16,19–25], amperometry [14], and quartz crystal microbalance [26]. However, the lifetime of DNA or antibodies in harsh conditions and their stability issues limit the practical application of these biosensors.

Nanomaterials are the leading cutting-edge research for the rapid development of point-of-care (POC) diagnostic tools due to their unique size-dependent properties, which make these materials superior and crucial in improving the patient's quality of life [27–29]. In particular, the use of gold nanoparticles is commonly exploited in biosensing applications due to their improved conductivity, biocompatibility, comparatively low toxicity, and improved analytical signal-to-noise ratio [22,30–33]. Antibiotics are also known as antibacterial agents, which are commonly used for the prevention and treatment of bacterial infections [34–38]. One of the frequently used antibiotics is amoxicillin trihydrate (AMX) for humans. The chemical structure of AMX is a form of β-lactam ring, which is purely responsible for the antibacterial, pharmacological, and chemical activities [34–38]. Recently, carbon nanomaterials and metal nanoparticle-modified carbon material-based electrochemical sensors and optical sensors for AMX have been extensively reviewed [34,36]. However, acute exposure to these antibiotics leaves residuals in the human body that can further increase resistant micro-organisms and antibiotic resistance. Thereby, the detection of AMX or residual AMX is important to understand the bacterial reaction, for instance, in one-step bulk construction of gold nanoparticles on multiwalled carbon nanotubes using electroless deposition for the electrochemical sensing of AMX in bovine milk samples [37]. Likewise, gold nanoparticle-modified mesoporous carbon nanomaterials have been used for the detection of AMX in mineral water and environmental water samples [38].

Among various carbon nanomaterials, carbon nanofibers (CNF) have the unique property of excellent conductivity, and its matrices with chitosan (CHIT) would make the hybrid composites more stable even in hydrodynamic conditions [31]. Likewise, gold nanostructures in hybrid with CHIT are highly stable for various electrocatalytic systems [31,32]. In this work, the interaction of amoxicillin (AMX, antibiotic drug) with Uropathogenic *E. coli* (UPEC) bacteria is monitored electrochemically for the first time. Nanostructured gold wires (AuNWs) are synthesized by using a chemical reduction method in which the morphology is controlled by appropriate gold nano seed and growth solutions in a suitable environment. The electrochemical antimicrobial resistance developed by UPEC on AMX sensing is taken as the key concept for the detection of pathogens by using a nanostructured gold wire (AuNW)-modified carbon nanofiber–chitosan (CNF-CHIT) matrix (Scheme 1). The synthesized AuNWs are characterized by scanning electron microscopy (SEM), UV-Visible spectrophotometry, and X-ray photoelectron spectroscopy (XPS). The CNF-CHIT/AuNW-modified system is also characterized by SEM and XPS to confirm the stability of the AuNWs.



Scheme 1. Cartoon for the CNF-CHIT/AuNW nanostructures toward the electrochemical sensing of AMX and AMX-assisted UPEC bacteria.

2. Materials and Methods

2.1. Materials

All the chemicals, such as gold (III) chloride trihydrate ($HAuCl_4 \cdot 3H_2O$), sodium citrate, sodium borohydride ($NaBH_4$), ascorbic acid, and amoxicillin trihydrate (AMX) antibiotic drug, were purchased from Sigma-Aldrich, St. Louis, MO, USA and Sisco Research Laboratories (SRL, Mumbai, India). Uropathogenic *E. coli* (UPEC) solution was purchased from SPECIALTY LAB & RESEARCH, Thanjavur, India, and stored in refrigerator at 4 °C. Bacteria chosen had inherent resistance towards amoxicillin, and the susceptibility was tested before purchase.

2.2. Instrumentations

The as-prepared AuNWs were characterized by scanning electron microscopy (TESCAN VEGA3, SEM), UV-Visible spectrophotometry (Perkin Elmer Lambda 35 UV-Visible Spectrometer), and X-ray photoelectron spectroscopy (Thermo scientific K-Alpha, XPS, Waltham, MA, USA). The electrochemical experiments were performed in electrochemical workstation (CHI600, CH instrument, Bee Cave, TX, USA) equipped with corresponding software.

2.3. Synthesis of Gold Nanowires

Gold nanowires (AuNWs) were synthesized using bottom-up approach by adopting the seeing method and appropriate aspect ratio-based growth solution (Figure 1a). Briefly, the seed solution was prepared by adding 0.2 mL of $HAuCl_4 \cdot 3H_2O$ (0.25 mM) to 19.8 mL of sodium citrate (0.25 mM) followed by dropwise addition of 1 mL $NaBH_4$ (0.1 M) to obtain a pink-colored solution. The growth solution was synthesized by mixture of 5 mL of $HAuCl_4 \cdot 3H_2O$ (0.25 mM) with 5 mL of 0.1 M of CTAB, and 0.1 M of ascorbic acid was added dropwise to the solution until the color changed. Then, the size-controlled AuNWs were prepared by dropwise addition of seed solution (1 mL) to the 5 mL of stock solution until obtaining stable pink-colored solution.

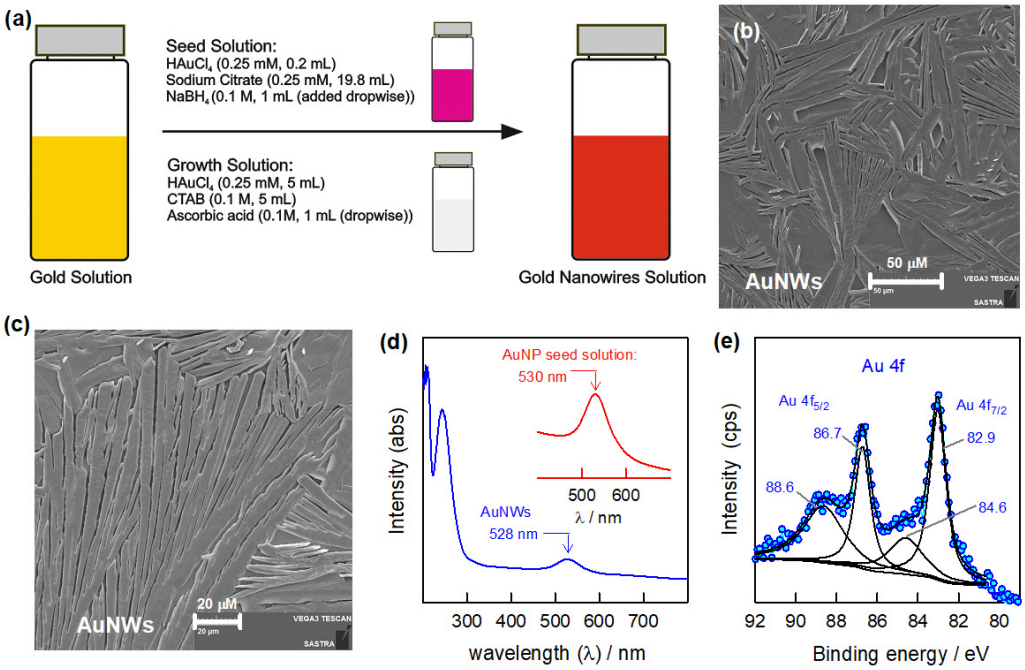


Figure 1. Schematic representation of the AuNW synthesis (**a**) along with characterizations: SEM images (**b**,**c**), UV-Visible spectroscopy (**d**), and XPS (**e**) analysis.

2.4. Electrochemical Experiments

Cyclic voltammetry (CV) and differential pulse voltammetry (DPV) were performed in the conventional three-electrode cell. Glassy carbon electrode was used as working electrode, Ag/AgCl as the reference electrode, and a platinum wire as the counter electrode. The pH 7 phosphate-buffered solution (0.1 M PBS) was used as supporting electrolyte. For the preparation of GCE/CNF-CHIT/AuNW-modified electrode, the cleaned GCE surface was functionalized using a composite mixture containing 400 µL of CNF-CHIT (50 mg of CNF in 400 µL of 5% chitosan) solution and 100 µL of the as-prepared AuNW solution. The whole mixture was shaken and mixed thoroughly, and then 5 µL of the final mixed composite solution was drop-casted onto the clean GCE surface and kept for drying at room temperature for 15 min. The as-obtained bacterial solution was added directly without dilution to the antibiotic-containing PB solution (10 mL) for their evaluation by DPV.

3. Results

3.1. Physicochemical Characterizations

The structural morphology was examined by SEM analysis (Figure 1b,c). The SEM images of the as-prepared AuNWs showed the long stretched wire-like structures of gold under different magnifications. It was further supported by UV-Visible analysis over the range of 200–800 nm (Figure 1d). The UV-Visible spectra of the gold seed solution and as-prepared AuNWs showed peaks at 530 nm and 528 nm, respectively [30,31]. The slight shift (~2 nm) in the observed peak indicates the formation of nanostructured gold particles with morphological changes. The presence of pure metallic gold nanostructures is confirmed by XPS studies (Figure 1e). As seen in the XPS spectra, the binding energies of the Au $4f_{7/2}$ and Au $4f_{5/2}$ peaks are clearly observed at 88.6 eV and 86.7 eV, and 84.6 eV and 82.9 eV, respectively, which corresponds to the pure metallic gold nanostructures [31]. The overall characterization studies confirm the formation of nanostructured gold wires is achieved successfully.

Further, the as-prepared AuNWs are mixed with CNF-CHIT matrices to improve the conductivity and stabilization of AuNWs for electrochemical sensing of AMX. The prepared mixture solution is also characterized by SEM analysis. The SEM images of the CNF-CHIT/AuNW mixture with two different magnifications are shown in Figure 2a,b. It is noticed that the

AuNWs are dispersed randomly on the CNF-CHIT matrix, which helps to retain the nature as well as the activities of each component. Furthermore, the core energy level XPS spectra of Au 4f, C 1s, N 1s, and O 1s of the CNF-CHIT/AuNWs system are displayed in Figure 2c–f. The observed binding energies of the Au $4f_{7/2}$ and Au $4f_{5/2}$ peaks at 89.1 eV and 87.1 eV, and 84.9 eV and 83.3 eV indicate the existence of metallic gold nanostructures [28]. The shift in the binding energies represents the interaction and stabilization of AuNWs within the CNF-CHIT matrices. The binding energies of C 1s are observed at 286.5 eV, 285.1 eV, and 283.3 eV, related to the O-C=O, C-OH/C-O-C, and C-C functional groups [28]. Likewise, the binding energies of the N 1s at 402.4 eV and 399.6 eV represent N-H and N-C < functionalities, while the O 1s at 533.6 eV, 532.8 eV, and 532.0 eV corresponds to the N-C=O, O=C=O, and C-OH/C-O-C functional groups present in the CNF-CHIT matrices [31]. From the SEM and XPS analysis, the as-synthesized AuNWs are well mixed and stabilized by CNF-CHIT functionalities purely in the presence of COOH and NH_2 functional groups. Furthermore, the CNF-CHIT/AuNWs are utilized for the electrochemical sensing of AMX and evaluating the antibacterial activities of UPEC bacteria.

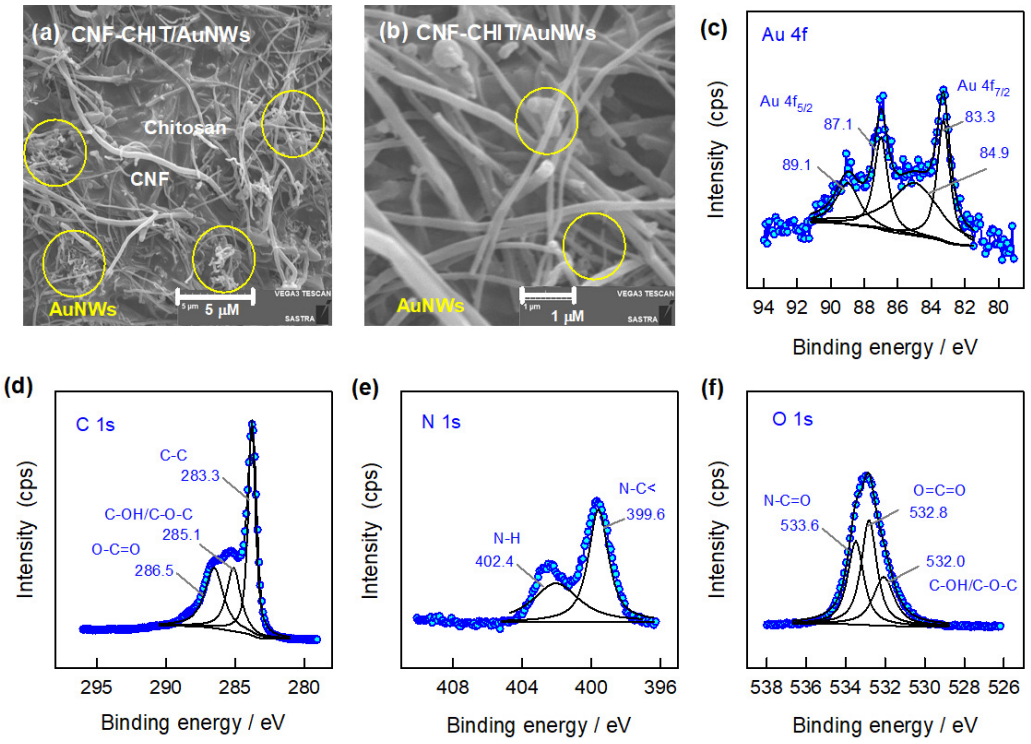


Figure 2. SEM images (**a**,**b**) and core energy level XPS spectra of Au 4f (**c**), C 1s (**d**), N 1s (**e**), and O 1s (**f**) of the CNF-CHIT/AuNWs system.

3.2. Electrochemical Sensing of AMX on GCE/CNF-CHIT/AuNWs

The electrochemical sensing of the AMX drug is studied by using CV and DPV techniques in pH 7 PBS (Figure 3). In order to understand the stability of the GCE/CNF-CHIT/AuNW-modified electrode, a continuous CV experiment was performed in blank pH 7 PBS at a scan rate of 50 mV s^{-1} in 0 to 1 V potential window (Figure 3a). Furthermore, the CV experiments are performed on the GCE/CNF-CHIT/AuNW-modified electrode in the presence and absence of amoxicillin (500 µM AMX) at a scan rate of 10 mV s^{-1} in the 0 to 1 V potential window (Figure 3b). The modified electrode showed an oxidation peak at 0.65 V vs. Ag/AgCl in the presence of the AMX drug. This observation confirms the electrochemical sensing of AMX in neutral pH conditions. Figure 3c represents the effect of various scan rates from 10 to 100 mV s^{-1} in the AMX solution resulting in the increasing current values (I) with respect to scan rates (v). The double logarithmic plot of log I vs. Log v showed good linearity (inset of Figure 3c). Furthermore, DPV experiments

on AMX sensing were performed under the same conditions. As seen in Figure 3d, the DPV current responses on the GCE/CNF-CHIT/AuNW electrode showed a linear increase with respect to the increase in the concentration of AMX. The concentration range of AMX is 25–600 μM. From the current values vs. concentration, a linear calibration plot was drawn (Figure 3e). The obtained calibration plot for AMX looks linear with a good regression value. There are two linear ranges, and the one from 25 to 325 μM is considered, probably due to the fact that it has a higher sensitivity. The calculated sensitivity value is 13.27 nA μM^{-1}. This observation reveals that the present CNF-CHIT/AuNWs is a model system for the electrochemical sensing of AMX. Once the system is working for a good linear range of AMX, it was preceded for further experiment. Figure 3f represents the possible electrochemical oxidation of AMX on the present CNF-CHIT/AuNW-modified electrode. From this conclusion, the UPEC bacterial reaction is preceded by monitoring the interaction of bacteria with AMX at a fixed concentration.

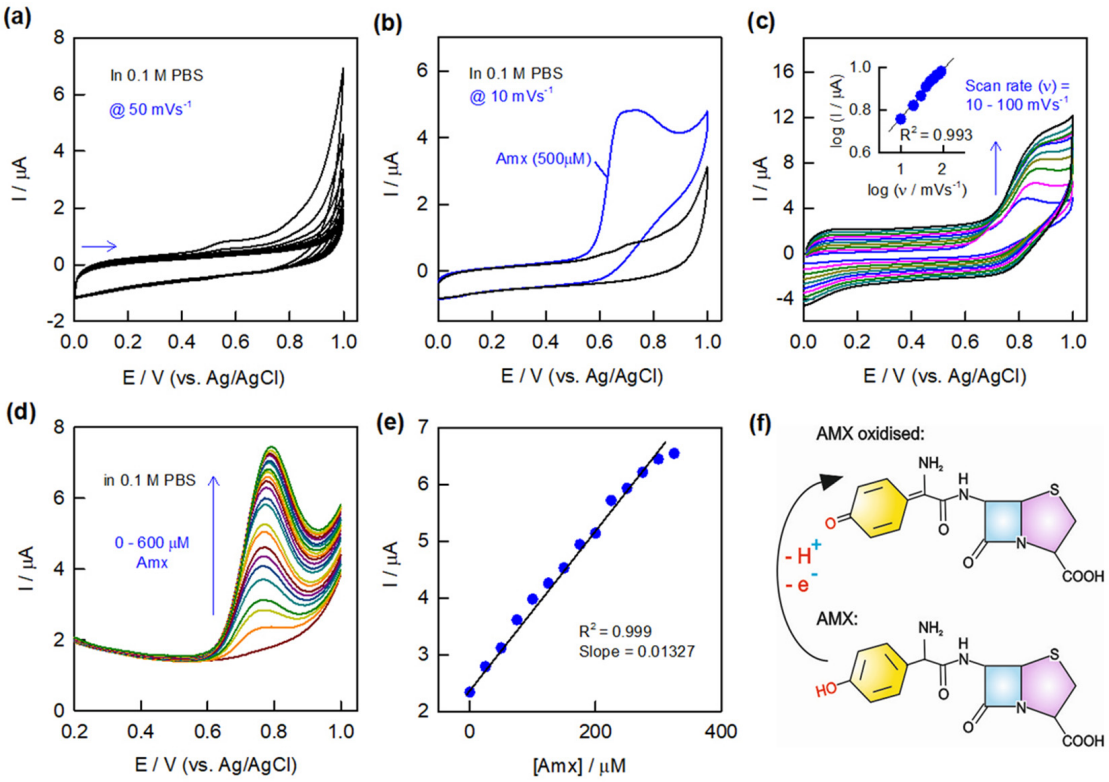


Figure 3. Continuous CV responses of GCE/CNF–CHIT/AuNWs in blank pH 7 PBS at a scan rate of 50 mV s^{-1} (**a**). CV responses of the stabilized modified electrode in the presence and absence of AMX (500 μM) at a scan rate of 10 mV s^{-1} (**b**) and effect of various CV scan rates along with double logarithmic plot (**c**) in pH 7 PBS. DPV responses of AMX in the range of 25–600 μM (**d**) along with the calibration plot (**e**). Possible mechanism for the electrochemical oxidation of AMX on the AuNW-modified electrode (**f**).

3.3. Electrochemical Evaluation of Antibacterial Activity

The bacterial species used in the experiment had inherent resistance to antibiotics [39]. The bacteria render the antibiotic ineffective by several mechanisms, and one of them is enzymatic activation, wherein the β-lactamase enzyme is released, which cleaves the β-lactam ring in the antibiotic [39,40]. The bacterial cell wall has peptidoglycans that give integrity to the cell and is maintained by two main enzymes: transglycosylase and transpeptidase. These enzymes help in cross-linking the peptidoglycan layers. The antibiotics containing β-lactam interfere with cell wall synthesis, which ultimately results in lysis of the cell. Penicillin derivative antibiotic is an analog of the D-alanyl-D-alanine dipeptide of peptidoglycan, which acts as a substrate for transpeptidase. The cross-linking of the peptidoglycans is inhibited by preventing the transpep-

tidase enzyme catalyzes. Thereby, it reduces the mechanical strength of the bacterial cell and hinders the cell wall synthesis process. In response to the stress, a few bacterial species release β-lactamase, which is an enzyme that recognizes the β-lactam ring present in the antibiotics and hydrolyzes the peptide bond present in the ring. Once the ring is open, the antibiotic becomes ineffective, and the bacterial species thrives. By taking advantage of this principle, the present work is designed for the evaluation of drug interaction on bacteria by electrochemical sensing of AMX.

The electrochemical evaluation of the antibacterial activity of the AMX antibiotic drug is shown, with respect to Uropathogenic *E. coli* (UPEC) bacteria, by the interaction of the drug with UPEC and the resistance developed by the bacteria towards the AMX antibiotic drug (Figure 4). The as-obtained bacterial solution was added directly in a specified quantity to the antibiotic solution, and the corresponding electrochemical activity was studied by DPV. At a fixed concentration of AMX (100 µM), different concentrations (0.6–1.2 × 10^6 CFU/mL) and different incubation times (1 h–1 h 35 min) were analyzed for bacterial reactions (Figure 4a,b). Prior to the bacterial reaction, the DPV experiment was performed for 100 µM AMX in 0.1 M PBS. After the addition of bacterial solution, the whole setup was left undisturbed for 1 h for incubation at room temperature in PBS, and then DPV was recorded. As seen in Figure 4a, the current response for the AMX decreased incrementally, and a prominent peak shift is also observed with different concentrations of bacterial solution. The potential peak shift may possibly be due to the immediate reaction of AMX with UPEC, whereas the incremental decrease in the current response is purely due to the interaction between them. Similarly, the effect of incubation time for the bacterial reaction was also studied under the same conditions (Figure 4b). It is observed that the increase in the incubation time leads to a further decrement in the AMX sensing current. This observation confirms the interaction of bacteria with the drug is still possible with respect to the changes in the peak potential followed by the decrease in the current responses. Figure 4c,d display the respective bar diagrams for the results obtained in the different concentrations of bacteria and the incubation time for the bacterial reaction with respect to the baseline corrected current values. The percentage value represents the decremental current values of the antibacterial reaction with respect to the AMX current value. As seen in the bar diagrams, the known concentration of AMX showed a constant current, which decreased gradually upon the addition of bacterial solution in terms of concentration and incubation time. Table 1 represents the summarized information about the versatile electrochemical sensing probes for the detection of the pathogen. From Table 1, we can conclude that the electrochemical sensing of pathogens was mainly demonstrated by DNA, antibody, aptamer, and peptide-based systems, unlike the antibacterial drug interaction-based detection system.

Table 1. Various electrochemical methodologies for sensing *E. coli* bacteria.

S. No	Pathogen	Electrode Modification	Methodology	Technique	Ref
1	*E. coli* O157:H7	Au/Thiol-modified methylene blue/ferrocene/DNA	DNA-based sensing	DPV	[12]
2	*E. coli*	Au/AuNP/3-mercaptopropyl-trimethoxysilane/DNA	DNA-based sensing	DPV	[13]
3	*E. coli* UTI	Au/biotin-modified capture probe/horseradish peroxidase (HRP)-conjugated anti-fluorescein antibody/RNA	DNA-based sensing	Amp *i-t*	[14]
4	*E. coli*	Gold–Tungsten/Streptavidin/Biotinylated anti-b-galactosidase	Antibody-based sensing	EIS	[15]
5	*E. coli* O157:H7	Indium–Tin oxide/EDC-NHS/ Anti-*E. coli*	Antibody-based sensing	EIS	[16]
6	*E. coli* O157:H7	SPCE/Fe_2O_3-Polyaniline/Antibody/AuNP/Antibody	Antibody-based sensing	DPV	[17]
7	*E. coli*	Au/Antibody/BSA/*E. coli*/Aptamer–primer probe	Aptamer-mediated sensing	DPV	[18]

Table 1. *Cont.*

S. No	Pathogen	Electrode Modification	Methodology	Technique	Ref
8	*E. coli* O157:H7	3D-interdigitated electrode/mercaptosilane/*E. coli* specific 5′disulfide-modified DNA aptamer	Aptamer-mediated sensing	EIS	[19]
9	*E. coli* O157:H7	Graphene-nitrocellulose/Thiolated 64-mer RNAaptamer/Antigen	Aptamer-mediated sensing	EIS	[20]
10	*E. coli* O78:K80:H11	SPE/Bridged Rebar Graphene/ Anti-*E. coli* aptamer	Aptamer-mediated sensing	EIS	[21]
11	*E. coli* O157:H7	Au/LipoicacidNHS/Ferrocene/ Antimicrobial peptides	Antimicrobial peptide-based sensing	EIS	[22]
12	*E. coli*	Au/11-mercapto-1-undecanoic acid/ dithiothreitol/Concanavalin A	Lectin-based sensing	EIS	[23]
13	*E. coli* K12	GCE/Polyethylenimine-CNT/ Bacteriophage	Bacteriophage-based sensing	EIS	[24]
14	*E. coli*	Au/3-((2, 5-dimethoxyphenyl)ethynyl) thiophene/α-D-Mannopyranoside, 2-[2-(2-mercaptoethoxy) ethoxy]ethyl	Carbohydrate-based sensing	EIS	[25]
15	UroPathogenic *E. coli* (UPEC)	GCE/CNF-CHIT/AuNWs	Antibacterial drug interaction-based sensing	DPV	This work

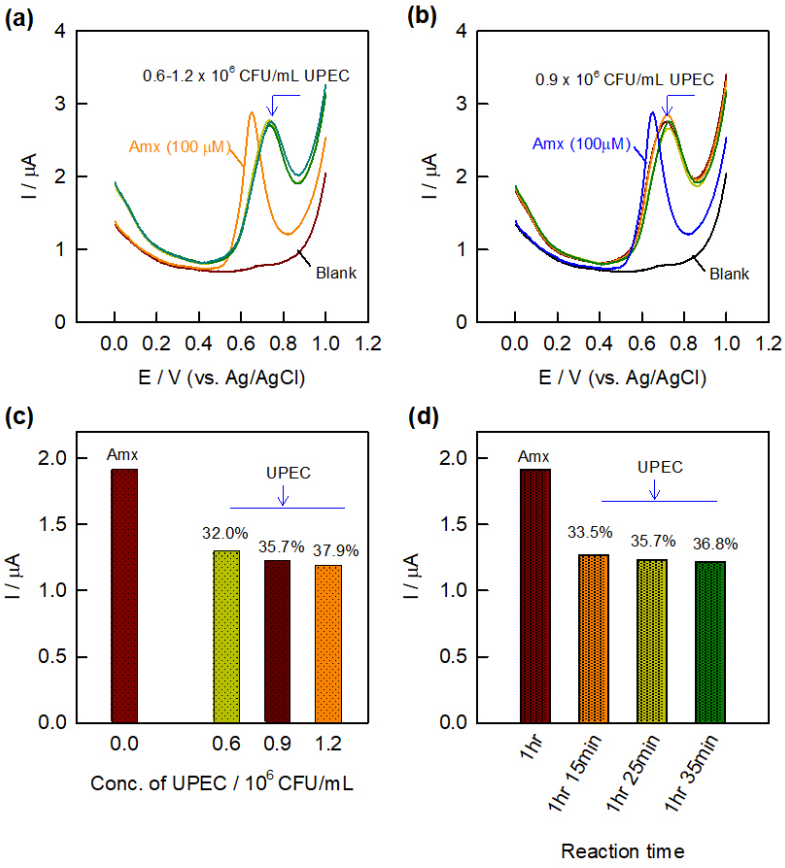


Figure 4. DPV response of different concentrations of UPEC bacteria (0.6–1.2 10^6 CFU/mL) (**a**) and different incubation times (1 h–1 h 35 min) (**b**) on GCE/CNF–CHIT/AuNWs in the presence of AMX (100 μM) along with respective bar diagrams (**c**,**d**).

4. Conclusions

The resistant behavior of bacterial species toward antibiotic drugs is the driving force for all the electrochemical experimental studies in this work. The present 'AMX and AMX-assisted UPEC' detection was demonstrated as a model system that can be extended to

achieve more specific and selective 'drug-pathogen' interaction studies. The developed CNF-CHIT/AuNW-modified electrode showed the current responses for sensing AMX in a linear range of 25–600 μM with a sensitivity value of 13.27 nA μM^{-1}. The conclusions arising from the present preliminary study are (i) after a specified incubation time, the bacteria begin to produce the enzyme which cleaves the antibiotic, thereby affecting the electron flow between the AMX and CNF-CHIT/AuNWs system, and (ii) after a particular incubation time, the electrochemical activity of the AMX is decreased due to the influence of β-lactamase enzyme. The more the bacterial concentration, the greater its impact, and hence, the current decreases with an increase in bacterial concentration as well as the incubation time. The present studies are helpful for the development of various specific and selective pathogen sensors with the aid of computational and theoretical approaches.

Author Contributions: J.S. performed the synthesis, characterizations, and experiments and prepared the first draft of the manuscript. S.N. conceptualized the idea, supervised, prepared the original draft, and corrected and revised the manuscript. All authors have read and agreed to the published version of the manuscript.

Funding: This research received no external funding.

Institutional Review Board Statement: Not applicable.

Informed Consent Statement: Not applicable.

Data Availability Statement: Not applicable.

Acknowledgments: The authors are grateful to the SASTRA Deemed University for the infrastructure and characterization facilities.

Conflicts of Interest: The authors declare no conflict of interest.

References

1. Foxman, B. The epidemiology of urinary tract infection. *Nat. Rev. Urol.* **2010**, *7*, 653–660. [CrossRef]
2. Karishetti, M.S.; Shaik, H.B. Clinicomicrobial assessment of urinary tract infections in a tertiary care hospital. *Indian J. Health Sci. Biomed. Res. (KLEU)* **2019**, *12*, 69.
3. Öztürk, R.; Murt, A. Epidemiology of urological infections: A global burden. *World J. Urol.* **2020**, *38*, 2669–2679. [CrossRef]
4. Tasoglu, S. Toilet-based continuous health monitoring using urine. *Nat. Rev. Urol.* **2022**, *19*, 219–230. [CrossRef]
5. Dospinescu, V.M.; Tiele, A.; Covington, J.A. Sniffing out urinary tract infection—Diagnosis based on volatile organic compounds and smell profile. *Biosensors* **2020**, *10*, 83. [CrossRef] [PubMed]
6. Flores-Mireles, A.L.; Walker, J.N.; Caparon, M.; Hultgren, S.J. Urinary tract infections: Epidemiology, mechanisms of infection and treatment options. *Nat. Rev. Microbiol.* **2015**, *13*, 269–284. [CrossRef]
7. Tan, C.W.; Chlebicki, M.P. Urinary tract infections in adults. *Singap. Med. J.* **2016**, *57*, 485. [CrossRef] [PubMed]
8. Najeeb, S.; Munir, T.; Rehman, S.; Hafiz, A.; Gilani, M.; Latif, M. Comparison of urine dipstick test with conventional urine culture in diagnosis of urinary tract infection. *J. Coll. Physicians Surg. Pak.* **2015**, *25*, 108–110. [PubMed]
9. Gennifer, T.S.; Dwork, N.; Khan, S.A.; Millet, M.; Magar, K.; Javanmard, M.; Bowden, A.K.E. Robust dipstick urinalysis using a low-cost, micro-volume slipping manifold and mobile phone platform. *Lab Chip* **2016**, *16*, 2069–2078.
10. Nellaiappan, S.; Mandali, P.K.; Prabakaran, A.; Krishnan, U.M. Electrochemical Immunosensors for Quantification of Procalcitonin: Progress and Prospects. *Chemosensors* **2021**, *9*, 182. [CrossRef]
11. Evtugyn, G.; Porfireva, A.; Shamagsumova, R.; Hianik, T. Advances in Electrochemical Aptasensors Based on Carbon Nanomaterials. *Chemosensors* **2020**, *8*, 96. [CrossRef]
12. Guo, Y.; Wang, Y.; Liu, S.; Yu, J.; Wang, H.; Liu, X.; Huang, J. Simultaneous voltammetric determination of *E. coli* and S. typhimurium based on target recycling amplification using self-assembled hairpin probes on a gold electrode. *Microchim. Acta* **2017**, *184*, 745–752. [CrossRef]
13. Redondo-Marugan, J.; Petit-Dominguez, M.; Casero, E.; Vázquez, L.; García, T.; Parra-Alfambra, A.; Lorenzo, E. Sol–gel derived gold nanoparticles biosensing platform for *Escherichia coli* detection. *Sens. Actuators B* **2013**, *182*, 307–314. [CrossRef]
14. Liao, J.C.; Mastali, M.; Gau, V.; Suchard, M.A.; Møller, A.K.; Bruckner, D.A.; Babbitt, J.T.; Li, Y.; Gornbein, J.; Landaw, E.M.; et al. Use of electrochemical DNA biosensors for rapid molecular identification of uropathogens in clinical urine specimens. *J. Clin. Microbiol.* **2006**, *44*, 561–570. [CrossRef]
15. Lu, L.; Chee, G.; Yamada, K.; Jun, S. Electrochemical impedance spectroscopic technique with a functionalized microwire sensor for rapid detection of foodbornepathogens. *Biosens. Bioelectron.* **2013**, *42*, 492–495. [CrossRef]
16. Yang, L.; Li, Y.; Erf, G.F. Interdigitated Array Microelectrode-Based Electrochemical Impedance Immunosensor for Detection of *Escherichia coli* O157: H7. *Anal. Chem.* **2004**, *76*, 1107–1113. [CrossRef]

17. Wang, Y.; Alocilja, E.C. Gold nanoparticle-labeled biosensor for rapid and sensitive detection of bacterial pathogens. *J. Biol. Eng.* **2015**, *9*, 16. [CrossRef]
18. Guo, Y.; Wang, Y.; Liu, S.; Yu, J.; Wang, H.; Wang, Y.; Huang, J. Label-free and highly sensitive electrochemical detection of *E. coli* based on rolling circle amplifications coupled peroxidase-mimicking DNAzyme amplification. *Biosens. Bioelectron.* **2016**, *75*, 315–319. [CrossRef]
19. Brosel-Oliu, S.; Ferreira, R.; Uria, N.; Abramova, N.; Gargallo, R.; Muñoz-Pascual, F.-X.; Bratov, A. Novel impedimetric aptasensor for label-free detection of *Escherichia coli* O157:H7. *Sens. Actuators B* **2018**, *255*, 2988–2995. [CrossRef]
20. Burrs, S.; Bhargava, M.; Sidhu, R.; Kiernan-Lewis, J.; Gomes, C.; Claussen, J.; McLamore, E. A paper based graphene-nanocauliflower hybrid composite for point of care biosensing. *Biosens. Bioelectron.* **2016**, *85*, 479–487. [CrossRef]
21. Kaur, H.; Shorie, M.; Sharma, M.; Ganguli, A.K.; Sabherwal, P. Bridged Rebar Graphene functionalized aptasensor for pathogenic *E. coli* O78:K80:H11 detection. *Biosens. Bioelectron.* **2017**, *98*, 486–493. [CrossRef]
22. Li, Y.; Afrasiabi, R.; Fathi, F.; Wang, N.; Xiang, C.; Love, R.; She, Z.; Kraatz, H.-B. Impedance based detection of pathogenic *E. coli* O157: H7 using a ferrocene-antimicrobial peptide modified biosensor. *Biosens. Bioelectron.* **2014**, *58*, 193–199. [CrossRef] [PubMed]
23. Yang, H.; Zhou, H.; Hao, H.; Gong, Q.; Nie, K. Detection of *Escherichia coli* with a label-free impedimetric biosensor based on lectin functionalized mixed self-assembled monolayer. *Sens. Actuators B* **2016**, *229*, 297–304. [CrossRef]
24. Zhou, Y.; Marar, A.; Kner, P.; Ramasamy, R.P. Charge-directed immobilization of bacteriophage on nanostructured electrode for wholecell electrochemical biosensors. *Anal. Chem.* **2017**, *89*, 5734–5741. [CrossRef] [PubMed]
25. Ma, F.; Rehman, A.; Liu, H.; Zhang, J.; Zhu, S.; Zeng, X. Glycosylation of quinone-fused polythiophene for reagentless and labelfree detection of *E. coli*. *Anal. Chem.* **2015**, *87*, 1560–1568. [CrossRef] [PubMed]
26. Jiang, A.X.; Wang, R.; Wang, Y.; Su, X.; Ying, Y.; Wang, J.; Li, Y. Evaluation of different micro/nanobeads used as amplifiers in QCM immunosensor for more sensitive detection of *E. coli* O157:H7. *Biosens. Bioelectron.* **2011**, *29*, 23–28. [CrossRef]
27. Dreaden, E.C.; Alkilany, A.M.; Huang, X.; Murphy, C.J.; El-Sayed, M.A. The golden age: Gold nanoparticles for biomedicine. *Chem. Soc. Rev.* **2012**, *41*, 2740–2779. [CrossRef]
28. Zumpano, R.; Polli, F.; D'Agostino, C.; Antiochia, R.; Favero, G.; Mazzei, F. Nanostructure-Based Electrochemical Immunosensors as Diagnostic Tools. *Electrochem* **2021**, *2*, 10–28. [CrossRef]
29. Facure, M.H.M.; Schneider, R.; Lima, J.B.S.; Mercante, L.A.; Correa, D.S. Graphene Quantum Dots-Based Nanocomposites Applied in Electrochemical Sensors: A Recent Survey. *Electrochem* **2021**, *2*, 490–519. [CrossRef]
30. Maurer, J.H.; González-García, L.; Reiser, B.; Kanelidis, I.; Kraus, T. Templated self-assembly of ultrathin gold nanowires by nanoimprinting for transparent flexible electronics. *Nano Lett.* **2016**, *16*, 2921–2925. [CrossRef]
31. Nellaiappan, S.; Kumar, A.S.; Nisha, S.; Pillai, K.C. In-situ preparation of Au(111) oriented nanoparticles trapped carbon nanofiber-chitosan modified electrode for enhanced bifunctional electrocatalysis and sensing of formaldehyde and hydrogen peroxide in neutral pH solution. *Electrochim. Acta* **2017**, *249*, 227–240. [CrossRef]
32. Almeida, L.A.; Rodrigues, B.V.M.; Balogh, D.T.; Sanfelice, R.C.; Mercante, L.A.; Frade-Barros, A.F.; Pavinatto, A. Chitosan/Gold Nanoparticles Nanocomposite Film for Bisphenol A Electrochemical Sensing. *Electrochem* **2022**, *3*, 239–247. [CrossRef]
33. Ito, Y.; Chang, T.-F.M.; Chien, Y.-A.; Chen, C.-Y.; Chakraborty, P.; Nakamoto, T.; Sone, M. Catalytic Activity of Atomic Gold-Decorated Polyaniline Support in Glucose Oxidation. *Electrochem* **2020**, *1*, 394–399. [CrossRef]
34. Hrioua, A.; Loudiki, A.; Farahi, A.; Bakasse, M.; Lahrich, S.; Saqrane, S.; El Mhammedi, M.A. Recent advances in electrochemical sensors for amoxicillin detection in biological and environmental samples. *Bioelectrochemistry* **2021**, *137*, 107687. [CrossRef]
35. Aihaiti, A.; Li, Z.; Qin, Y.; Meng, F.; Li, X.; Huangfu, Z.; Chen, K.; Zhang, M. Construction of electrochemical sensors for antibiotic detection based on carbon nanocomposites. *Nanomaterials* **2022**, *12*, 2789. [CrossRef] [PubMed]
36. Zahra, Q.A.; Luo, Z.; Ali, R.; Khan, M.I.; Li, F.; Qiu, B. advances in gold nanoparticles-based colorimetric aptasensors for the detection of antibiotics: An overview of the past decade. *Nanomaterials* **2021**, *11*, 840. [CrossRef] [PubMed]
37. Muhammad, A.; Yusof, N.A.; Hajian, R.; Abdullah, J. Construction of an electrochemical sensor based on carbon nanotubes/gold nanoparticles for trace determination of amoxicillin in bovine milk. *Sensors* **2016**, *16*, 56. [CrossRef]
38. Pollap, A.; Knihnicki, P.; Kus'trowski, P.; Kozak, J.; Cezpa, M.G.; Kotarba, A.; Kochana, J. Sensitive voltammetric amoxicillin sensor based on tio2 sol modified by cmk-3-type mesoporous carbon and gold ganoparticles. *Electroanalysis* **2018**, *30*, 2386–2396. [CrossRef]
39. Ahmed, N.; Khalid, H.; Mushtaq, M.; Basha, S.; Rabaan, A.A.; Garout, M.; Halwani, M.A.; Mutair, A.A.; Alhumaid, S.; Alawi, Z.A.; et al. The molecular characterization of virulence determinants and antibiotic resistance patterns in human bacterial uropathogens. *Antibiotics* **2022**, *11*, 516. [CrossRef]
40. Gupta, K.; Bhadelia, N. Management of urinary tract infections from multidrug-resistant organisms. *Infect. Dis. Clin.* **2014**, *28*, 49–59. [CrossRef]

Disclaimer/Publisher's Note: The statements, opinions and data contained in all publications are solely those of the individual author(s) and contributor(s) and not of MDPI and/or the editor(s). MDPI and/or the editor(s) disclaim responsibility for any injury to people or property resulting from any ideas, methods, instructions or products referred to in the content.